Figure S1

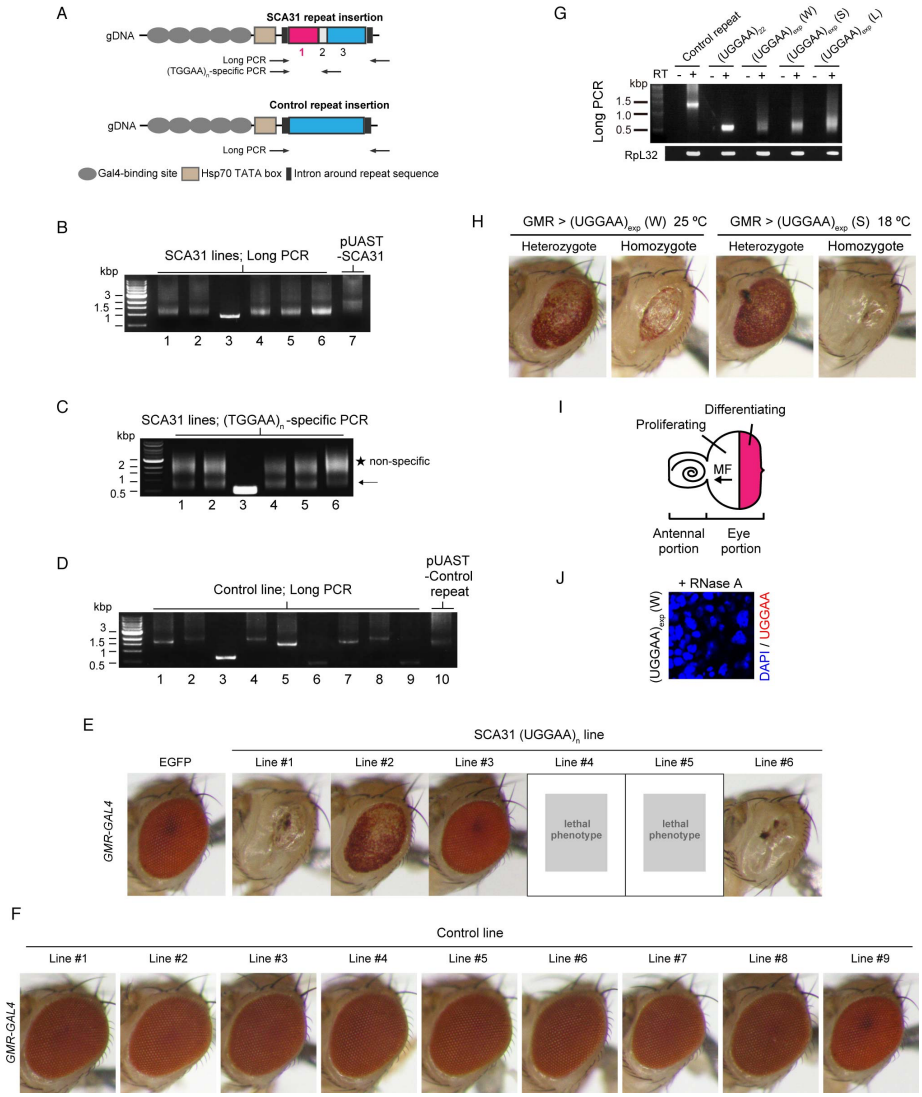

Figure S1. Characterization of the fly lines, Related to Figure 1

(A) Schematic of the constructs and positions of the two primer sets for SCA31 and control fly lines. (B–D) Estimation of the size of the insertion fragments (B, D) and the SCA31-specific TGGAA repeat sequence (arrow in C, magenta in A), by long PCR and TGGAA-specific PCR, respectively. (E) Light microscopy images of compound eyes from *Drosophila* expressing EGFP (control), line #1 (strong expression), line #2 (weak expression), line #3 (22 repeats) and line #6 (strong expression) using *GMR-Gal4*. Lines #4 and #5 were pupal lethal. (F) Light microscopy images of compound eyes of control repeat fly lines (Control #1–9). (G) Reverse-transcription PCR analysis of transgene expression of the transgenic fly lines. RpL32 was used as an internal standard. (H) Images of the disrupted eye morphology of homozygous and heterozygous $UGGAA_{exp}$ (W) flies at 25 °C and $UGGAA_{exp}$ (S) flies at 4 °C. Genotypes: heterozygote: GMR-GAL4/y; UAS-$UGGAA_{exp}$ (W)/UAS-EGFP; homozygote: GMR-GAL4/y; UAS-$UGGAA_{exp}$ (W)/UAS-$UGGAA_{exp}$ (W); heterozygote: GMR-GAL4/y; UAS-$UGGAA_{exp}$ (S)/UAS-EGFP; and homozygote: GMR-GAL4/y; UAS-$UGGAA_{exp}$ (S)/UAS-$UGGAA_{exp}$ (S). (I) Schematic of the eye imaginal fly disc. Photoreceptor differentiation occurred in the eye imaginal discs of third-instar larvae, and the *GMR-GAL4* system drives transgene expression only in the differentiating photoreceptors. (J) Specificity of the FISH probe was confirmed by treatment of the tissues with RNase, which diminished RNA foci.

Figure S2

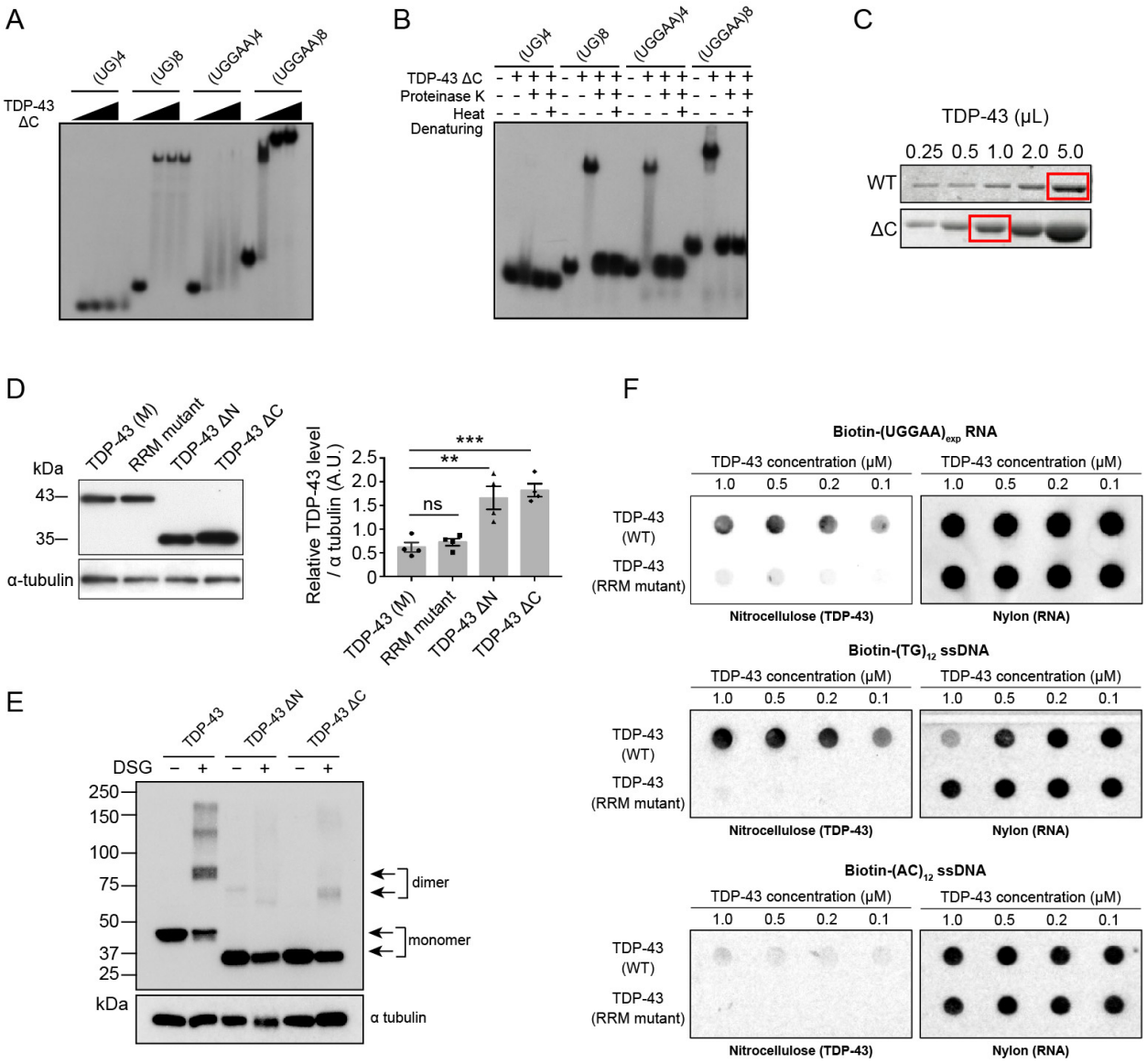

Figure S2. Expression of TDP-43 variants, Related to Figure 2 and 3

(A) Binding of RNA oligonucleotides to increasing amounts of TDP-43 ΔC. (B) Heat denaturation and/or proteinase K treatment abolishes TDP-43 ΔC binding to RNA oligos, which then comigrate with unbound RNA. Human recombinant TDP-43 WT and TDP-43 ΔC and [γ-^{32}P] ATP end-labeled r(UG)n and r(UGGAA)n (where n=4 or 8) were incubated for 30 min at room temperature in buffer containing 10 mM Tris pH 8, 10 mM NaCl, 2 mM $MgCl_2$, 5% glycerol and 1 mM DTT. Where indicated, proteinase K (2 μg/μL) was added and incubated for 10 min at 37 °C and heat denaturing was performed for 2 min at 85 °C. Samples were run on a 6% polyacrylamide gel for 2 h at 120 V (9 V/cm). (C) Relative amounts of TDP-43 WT & TDP-43 ΔC were standardized in EMSAs using SDS-PAGE gels with Coomassie staining to determine that TDP-43 ΔC should be diluted 1:5 prior to the binding experiments, as indicated by the red boxes. (D) Immunoblots showing the expression of TDP-43 variants in the fly lines. Data are presented as mean ± SEM, p = 0.0001, one-way ANOVA, **p < 0.01, ***p < 0.001, Dunnett's *post hoc* analysis; n.s. indicates no significant difference.

(E) The five fly heads were treated with DSG, a homobifunctional NHS-ester crosslinking reagent used to study native protein structures. Immunoblot analysis revealed that TDP-43 in noncrosslinked fly tissues expressing TDP-43 WT, ΔC or ΔN migrates at a speed corresponding to the expected molecular weight of a monomer (43 or 35 kDa),

whereas TDP-43 in DSG-treated fly tissues except for ΔN expression migrates at a speed corresponding to the expected molecular weight of a homodimer (86 kDa). (F) Filter binding assay using biotinylated single-stranded DNA or *in vitro*-transcribed UGGAA repeat RNA (20 repeat units or more) as a substrate for TDP-43 WT and TDP-43 RRM mutant proteins. A nitrocellulose membrane traps proteins including DNA-bound and unbound TDP-43, whereas unbound DNAs are recovered on a nylon membrane. *B*, Here, 6 ng/μL biotinylated UGGAA repeat RNA, 0.1 μM biotinylated (TG)12 (*middle*) or biotinylated (AC)12 (*lower*) was mixed with TDP-43 (wild type as well as RRM mutant) at the indicated concentrations. These mixtures were filtered through a nitrocellulose membrane (*left*) overlaid on a nylon membrane (*right*), and nucleic acids trapped on each of the membranes were probed with Streptavidin-HRP.

Figure S3

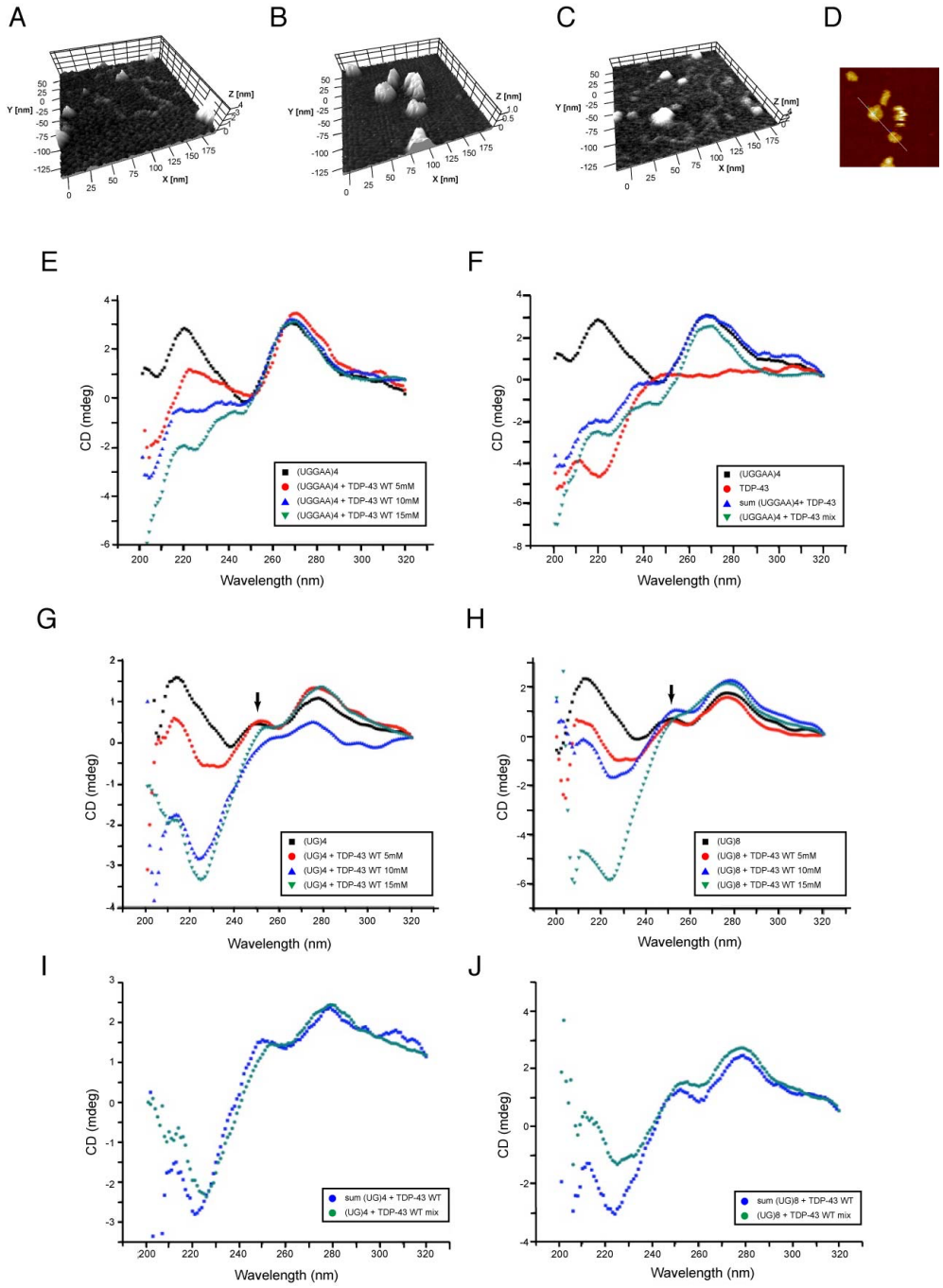

Figure S3. AFM images of the UGGAA$_{exp}$ RNA solution and CD spectra of UGGAA or UG repeat RNA, Related to Figure 4

(A–C) Representative three-dimensional AFM images of UGGAA$_{exp}$ RNAs in solution. Immediately after denaturation of the RNAs, many single-stranded RNAs with an estimated height of approximately 0.9 nm or less were observed (A). However, after 10 min of incubation at room temperature, RNAs tended to form large RNA aggregates with a height of over 2.5 nm (B). In contrast, in the solution with both TDP-43 ΔC and UGGAA$_{exp}$ RNA (C), UGGAA$_{exp}$ tended to remain as single strands. (D) Height analysis of UGGAA RNA aggregates in Figure 4F was performed using this image, which is adjusted to a lower intensity for accurate measurement. Scale bars = 50 nm.

CD spectra of UGGAA or UG repeat RNA

(E) CD titration of 8 μM (UGGAA)4 with aliquots of TDP-43 [0 mM (black), 5 mM (red), 10 mM (blue) and 15 mM (green)]. Green plot corresponds to the highest concentration of TDP-43. (F) CD spectra of (UGGAA)4 alone, TDP-43 alone, the sum of spectra obtained from TDP-43 and (UGGAA)4 separately and the spectrum obtained from incubating them together corresponding to (UGGAA)4+TDP-43 binding. (G) CD titration of 20 μM (UG)4 and (H) (UG)8 with aliquots of TDP-43. Green plot corresponds to the highest concentration of TDP-43. (I) The sum of CD spectra obtained from TDP-43 and (UG)4 separately and the spectrum obtained from incubating them together corresponding to (UG)4+TDP-43 binding. (J) The sum of CD spectra obtained from TDP-43 and (UG)8 separately and the spectrum obtained from incubating them together corresponding to (UG)8+TDP-43 binding.

Figure S4

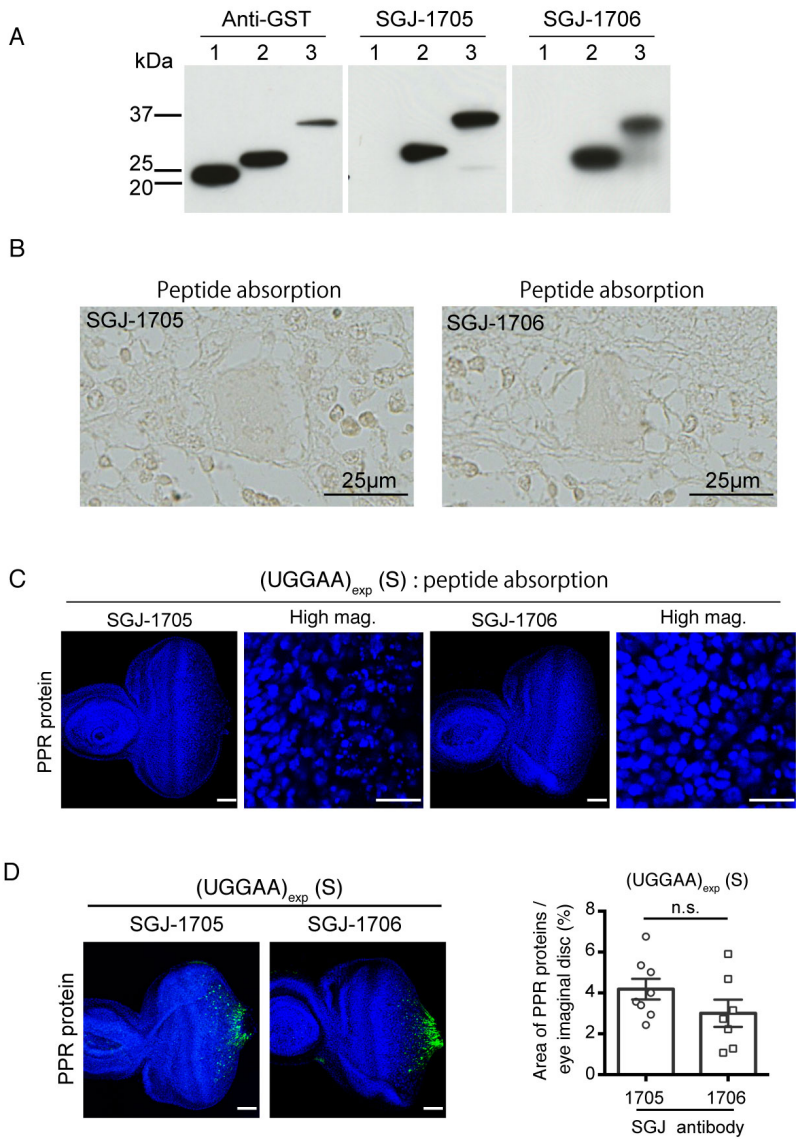

Figure S4. Characterization of anti-PPR antibodies, Related to Figure 5

(A) Immunoblot analyses confirmed the specificity of anti-PPR antibodies using recombinant proteins generated in *Escherichia coli*. Lane 1: GST only; lane 2: PPR proteins derived from the $(TGGAA)_{25}$ repeat DNA; lane 3: PPR proteins derived from the $(TGGAA)_{57}$ repeat DNA. (B–C) The level of PPR proteins detected by the two antibodies diminished upon antigen preabsorption in SCA31 human brain and fly tissue. Scale bars = 50 or 10 μm (high mag.). (D) The PPR proteins were detected in the eye imaginal discs of third-instar $(UGGAA)_{exp}$ (S) fly larvae using *GMR-GAL4* by both SGJ-1705 and SGJ-1706 antibodies. No statistically significant difference was observed in the area of PPR proteins detected by the two antibodies Data are presented as mean ± SEM, n =7-8 per genotype, p = 0.1766, two-tailed unpaired Student's t-test, n.s. indicates no significant difference.

Figure S5

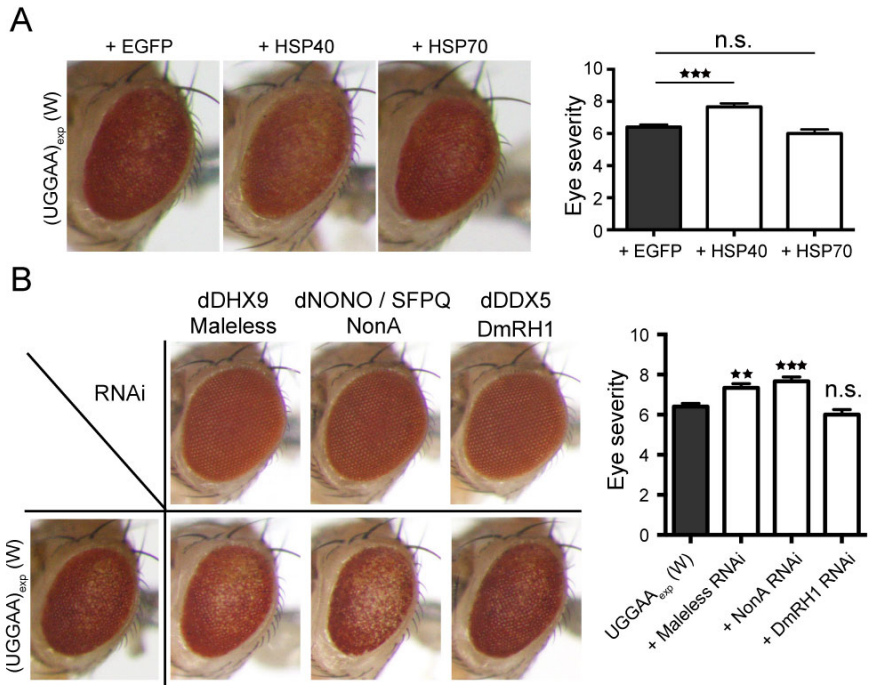

Figure S5. Molecular chaperones fail to rescue UGGAA$_{exp}$-mediated toxicity, Related to Figure 5

(A) Light microscopy images with eye degeneration scores of the flies of the indicated genotypes (means ± S.E.M.; **p* < 0.05, one-way ANOVA; n = 6–8 per genotype; NS indicates no significant difference). Coexpression of HSP40 and HSP70 did not suppress UGGAA$_{exp}$-mediated toxicity, suggesting that the pathomechanism of UGGAA$_{exp}$-mediated toxicity may differ from that caused by expanded CGG repeats in the FXTAS fly model. (B) Light microscopy images with eye degeneration scores of the flies of the indicated genotypes (n=6-10). Data are presented as mean ± SEM, p = 0.0001, one-way ANOVA, ***p = 0.0005, p = 0.2915, Dunnett's *post hoc* analysis, n.s., not significant.

Depletion of proteins that potentially bind to UGGAA$_{exp}$, such as dDHX9 and dNONO/SFPQ, exacerbated eye degeneration in flies expressing UGGAA$_{exp}$, suggesting that these proteins may also contribute to the pathogenesis of compound eye degeneration. Knockdown of dDDX5 did not cause significant changes in the eye morphology of flies expressing UGGAA$_{exp}$ (W). Data are presented as mean ± SEM, p < 0.0001, one-way ANOVA, **p = 0.0077, ***p = 0.0004, p = 0.3643, Dunnett's *post hoc* analysis, n.s., not significant.

Figure S6

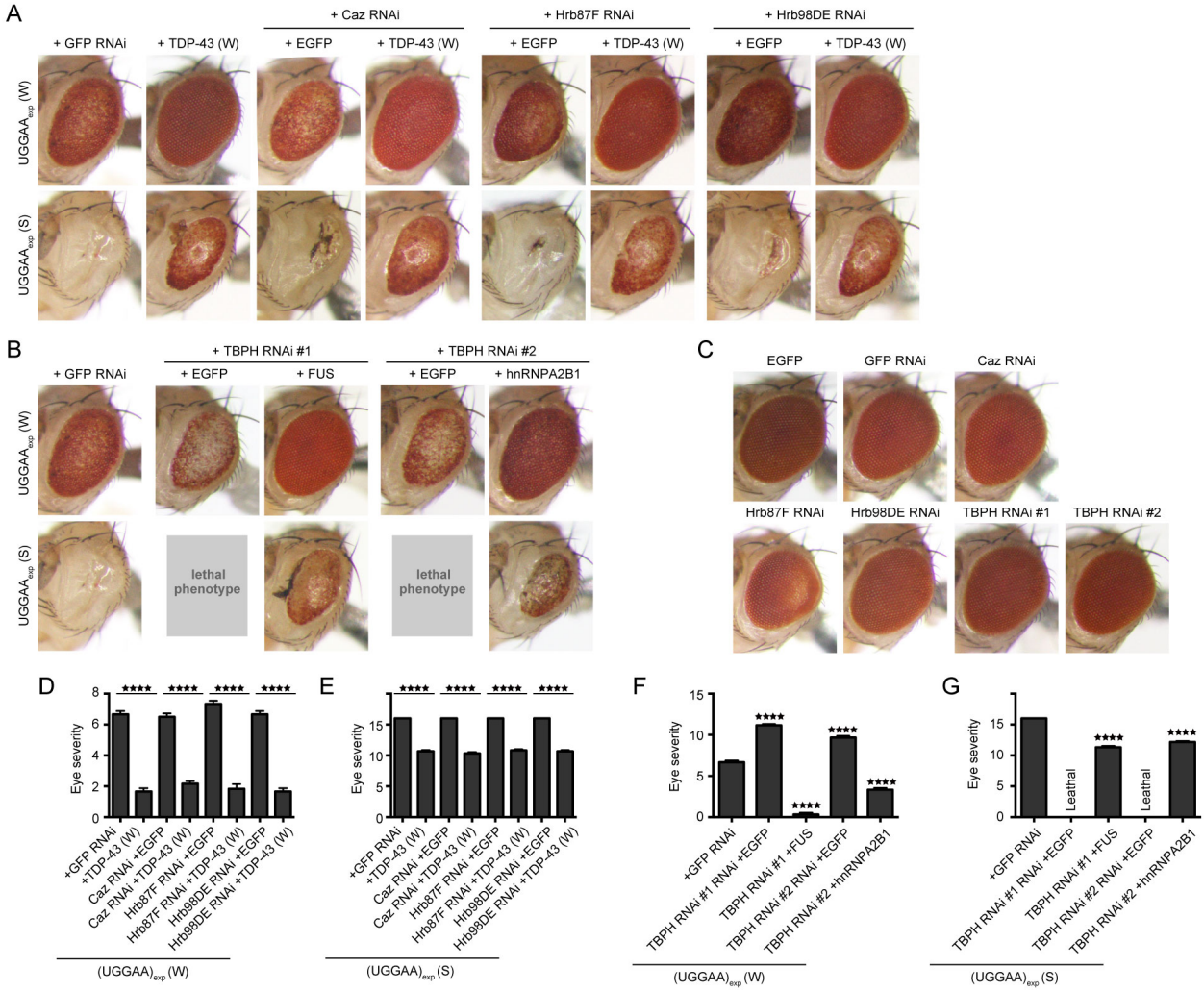

Figure S6. TDP-43, FUS and hnRNPA2B1 can act independently to suppress UGGAA$_{exp}$-induced toxicity, Related to Figure 6

(A–C) Representative compound eye images of 1–3-day-old flies of the indicated genotypes. Silencing of Caz, Hrb87F or Hrb98DE did not prevent TDP-43-mediated suppression of UGGAA$_{exp}$-induced toxicity. Likewise, knockdown of TBPH did not affect the FUS- or hnRNPA2B1-mediated suppression of UGGAA$_{exp}$-induced toxicity *in Drosophila.* (D–G) The quantification of eye severity of the indicated fly genotypes (n = 6-10). Data are presented as mean ± SEM, $p < 0.0001$, one-way ANOVA, ****$p < 0.0001$, Dunnett's *post hoc* analysis, n.s., not significant.

Figure S7

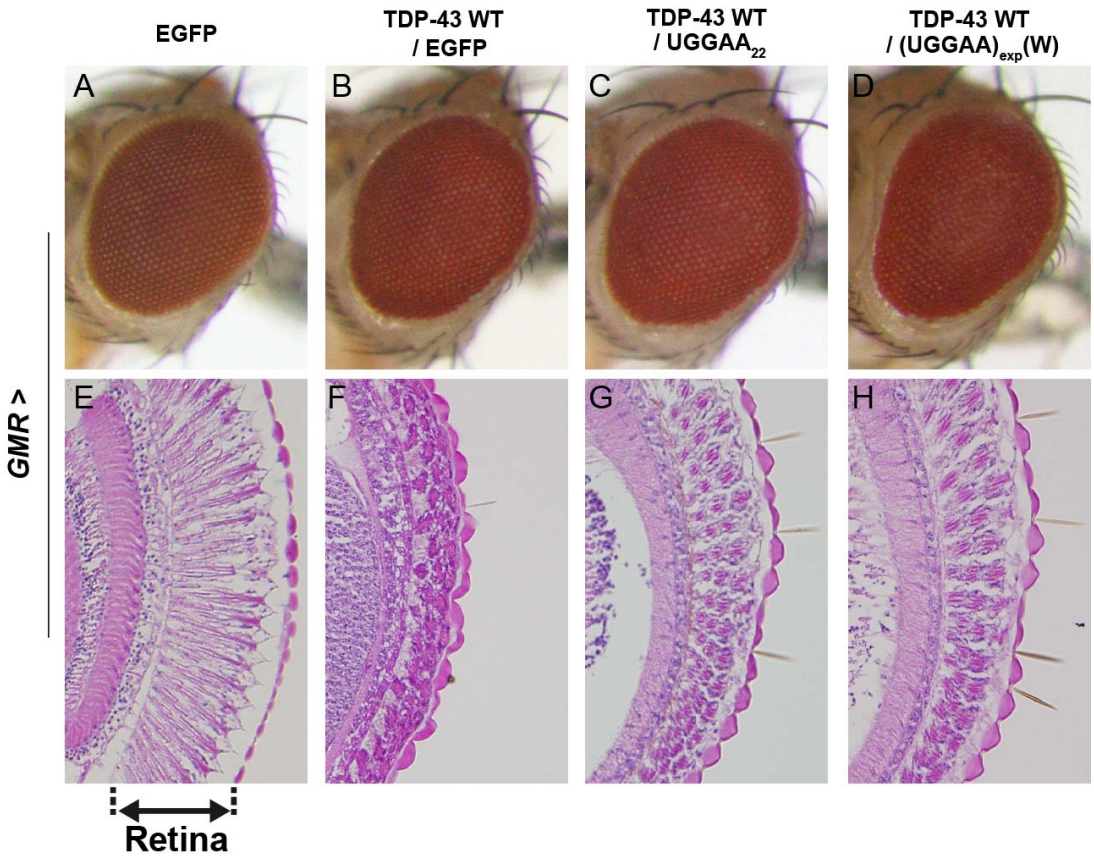

Figure S7. Beneficial effect of interaction between repetitive UGGAA RNA and TDP-43, Related to Figure 7
(A–D) Representative compound eye images of 1–3-day-old flies of the indicated genotypes. (E–H) Retinal cryosections of eyes of 1–3-day-old flies. TDP-43 WT expression in Drosophila by the eye-specific GMR-GAL4 driver causes thinning of the retina (F). However, coexpression of nontoxic short UGGAA, UGGAA22 (G) or relatively low-level expression of long UGGAA (H) leads to the restoration of retinal thickness in compound eyes.

Table S1. Fly Phenotypes, Related to Figure 1

Fly line / Driver line	Weak (Line 2)	Strong (Line 1, 6)	Lethal (Line 4, 5)	Short repeat (Line 3)
GMR-GAL4 (eye and other tissues including brain, trachea, and wing discs)	Rough eye Loss of pigmentation	Severe degeneration and loss of pigmentation Pupa semi-lethal	Pupa lethal	Normal
ELAV-GAL4 (all neuronal cells)	Short life span	Pupa lethal	Pupa lethal	Normal

Table S2. Identification of Proteins Associated with Expanded UGGAA Repeats, Related to Figure 2

Accession	Description	Score	Coverage	# Peptides	# PSM	# AAs	MW [kDa]	calc. pI
Q9D0E1	Heterogeneous nuclear ribonucleoprotein M [HNRPM_MOUSE]	614.77	34.16	21	150	729	77.6	8.63
O35737	Heterogeneous nuclear ribonucleoprotein H [HNRH1_MOUSE]	566.30	46.99	14	115	449	49.2	6.30
P70333	Heterogeneous nuclear ribonucleoprotein H2 [HNRH2_MOUSE]	535.12	46.99	13	106	449	49.2	6.30
P09405	Nucleolin [NUCL_MOUSE]	365.78	29.84	22	80	707	76.7	4.75
Q8R081	Heterogeneous nuclear ribonucleoprotein L [HNRPL_MOUSE]	361.80	34.30	13	81	586	63.9	8.10
Q8C854	Myelin expression factor 2 [MYEF2_MOUSE]	287.99	29.27	16	74	591	63.3	8.87
P42669	Transcriptional activator protein Pur-alpha [PURA_MOUSE]	265.77	41.43	9	50	321	34.9	6.44
O88569	Heterogeneous nuclear ribonucleoproteins A2/B1 [ROA2_MOUSE]	256.36	29.46	10	52	353	37.4	8.95
Q921F2	TAR DNA-binding protein 43 [TADBP_MOUSE]	251.17	33.57	10	56	414	44.5	6.70
Q8VEK3	Heterogeneous nuclear ribonucleoprotein U [HNRPU_MOUSE]	217.95	21.75	14	43	800	87.9	6.24
Q91VM5	Heterogeneous nuclear ribonucleoprotein G-like 1 [RBMXL_MOUSE]	188.02	22.16	9	44	388	42.1	9.99
P56959	RNA-binding protein FUS [FUS_MOUSE]	181.97	12.36	8	42	518	52.6	9.36
Q8BG05	Heterogeneous nuclear ribonucleoprotein A3 [ROA3_MOUSE]	165.92	30.61	15	34	379	39.6	9.01
O35295	Transcriptional activator protein Pur-beta [PURB_MOUSE]	148.48	42.28	9	29	324	33.9	5.43
Q8VIJ6	Splicing factor, proline- and glutamine-rich [SFPQ_MOUSE]	147.89	17.60	9	32	699	75.4	9.44
Q60668	Heterogeneous nuclear ribonucleoprotein D0 [HNRPD_MOUSE]	139.83	23.38	10	31	355	38.3	7.81
Q9Z2X1	Heterogeneous nuclear ribonucleoprotein F [HNRPF_MOUSE]	138.90	28.92	6	28	415	45.7	5.49
Q99K48	Non-POU domain-containing octamer-binding protein [NONO_MOUSE]	116.01	32.14	8	28	473	54.5	8.95
Q91VR5	ATP-dependent RNA helicase DDX1 [DDX1_MOUSE]	110.76	36.62	18	24	740	82.4	7.21
Q7TMK9	Heterogeneous nuclear ribonucleoprotein Q [HNRPQ_MOUSE]	108.79	24.08	11	26	623	69.6	8.59
P49312	Heterogeneous nuclear ribonucleoprotein A1 [ROA1_MOUSE]	91.87	25.00	6	20	320	34.2	9.23
Q91W50	Cold shock domain-containing protein E1 [CSDE1_MOUSE]	84.69	18.17	10	18	798	88.7	6.37
Q8VHK9	Probable ATP-dependent RNA helicase DHX36 [DHX36_MOUSE]	83.61	16.78	11	18	1001	113.8	8.41
Q7TMM9	Tubulin beta-2A chain [TBB2A_MOUSE]	78.50	45.17	13	18	445	49.9	4.89
O35286	Putative pre-mRNA-splicing factor ATP-dependent RNA helicase DHX15 [DHX15_MOUSE]	76.47	20.75	13	18	795	90.9	7.46
P99024	Tubulin beta-5 chain [TBB5_MOUSE]	73.87	49.10	13	17	444	49.6	4.89
Q8VDM6	Heterogeneous nuclear ribonucleoprotein U-like protein 1 [HNRL1_MOUSE]	72.39	18.04	8	13	859	95.9	6.58
Q9ERD7	Tubulin beta-3 chain [TBB3_MOUSE]	68.86	27.56	9	16	450	50.4	4.93
Q6NVF9	Cleavage and polyadenylation specificity factor subunit 6 [CPSF6_MOUSE]	66.76	15.06	6	13	551	59.1	7.15
P47857	6-phosphofructokinase, muscle type [K6PF_MOUSE]	64.50	19.62	11	13	780	85.2	8.00
P11798	Calcium/calmodulin-dependent protein kinase type II subunit alpha [KCC2A_MOUSE]	64.14	22.18	7	14	478	54.1	7.08
Q6IFX2	Keratin, type I cytoskeletal 42 [K1C42_MOUSE]	63.75	9.29	3	15	452	50.1	5.16
P32067	Lupus La protein homolog [LA_MOUSE]	62.95	28.43	9	14	415	47.7	9.77
Q8R326	Paraspeckle component 1 [PSPC1_MOUSE]	57.22	20.27	6	11	523	58.7	6.67
P24547	Inosine-5'-monophosphate dehydrogenase 2 [IMDH2_MOUSE]	52.82	22.76	10	11	514	55.8	7.28
Q6PDM2	Serine/arginine-rich splicing factor 1 [SRSF1_MOUSE]	51.76	32.66	8	14	248	27.7	10.36
Q9CQF3	Cleavage and polyadenylation specificity factor subunit 5 [CPSF5_MOUSE]	49.58	39.21	6	10	227	26.2	8.82
Q9WUA3	6-phosphofructokinase type C [K6PP_MOUSE]	47.38	17.73	8	9	784	85.4	7.11
Q9JIK5	Nucleolar RNA helicase 2 [DDX21_MOUSE]	45.08	15.63	9	11	851	93.5	9.11
Q99020	Heterogeneous nuclear ribonucleoprotein A/B [ROAA_MOUSE]	44.11	15.79	5	11	285	30.8	7.91
P28652	Calcium/calmodulin-dependent protein kinase type II subunit beta [KCC2B_MOUSE]	41.16	18.27	6	9	542	60.4	7.28
Q99LF4	tRNA-splicing ligase RtcB homolog [RTCB_MOUSE]	40.91	20.59	8	10	505	55.2	7.23
Q9Z130	Heterogeneous nuclear ribonucleoprotein D-like [HNRDL_MOUSE]	39.54	26.25	7	9	301	33.5	7.31
Q921M3	Splicing factor 3B subunit 3 [SF3B3_MOUSE]	39.07	8.46	7	9	1217	135.5	5.26
Q497V5	S1 RNA-binding domain-containing protein 1 [SRBD1_MOUSE]	36.49	7.68	6	9	1015	114.0	8.78
Q9JJ43	RNA binding protein fox-1 homolog 1 [RFOX1_MOUSE]	36.33	11.11	3	8	396	42.7	6.86
P16381	Putative ATP-dependent RNA helicase Pl10[DDX3L_MOUSE]	35.40	10.91	6	8	660	73.1	7.18
Q00PI9	Heterogeneous nuclear ribonucleoprotein U-like protein 2 [HNRL2_MOUSE]	32.93	8.32	6	7	745	84.9	4.89
Q9DBR1	5'-3' exoribonuclease 2 [XRN2_MOUSE]	32.25	7.78	5	8	951	108.6	7.59
P60824	Cold-inducible RNA-binding protein [CIRBP_MOUSE]	31.71	27.91	3	6	172	18.6	9.61
P62960	Nuclease-sensitive element-binding protein 1 [YBOX1_MOUSE]	30.44	29.50	4	5	322	35.7	9.88
Q8BYK6	YTH domain family protein 3 [YTHD3_MOUSE]	30.08	8.03	3	7	585	63.9	9.04
Q9Z1Z2	Serine-threonine kinase receptor-associated protein [STRAP_MOUSE]	29.52	18.86	4	6	350	38.4	5.12
Q9CQE8	UPF0568 protein C14orf166 homolog [CN166_MOUSE]	29.18	36.48	6	7	244	28.1	6.89
P62996	Transformer-2 protein homolog beta [TRA2B_MOUSE]	28.91	10.42	2	6	288	33.6	11.25
Q8C5Q4	G-rich sequence factor 1 [GRSF1_MOUSE]	28.45	13.57	4	6	479	53.0	6.67
Q3U0V1	Far upstream element-binding protein 2 [FUBP2_MOUSE]	27.97	11.63	5	7	748	76.7	7.33
P63017	Heat shock cognate 71 kDa protein [HSP7C_MOUSE]	26.66	11.61	5	6	646	70.8	5.52
Q6P3D0	U8 snoRNA-decapping enzyme [NUD16_MOUSE]	25.96	27.69	5	6	195	21.8	7.12
Q6A0A9	Constitutive coactivator of PPAR-gamma-like protein 1 [F120A_MOUSE]	25.75	8.09	6	6	1112	121.6	8.92
Q8BIF2	RNA binding protein fox-1 homolog 3 [RFOX3_MOUSE]	24.44	13.10	3	5	374	40.6	7.90
Q61656	Probable ATP-dependent RNA helicase DDX5 [DDX5_MOUSE]	23.77	7.82	4	6	614	69.2	8.92
Q9CZU3	Superkiller viralicidic activity 2-like 2 [SK2L2_MOUSE]	23.52	6.92	6	6	1040	117.6	6.40
Q9DBC3	Cap-specific mRNA (nucleoside-2'-O-)-methyltransferase 1 [MTR1_MOUSE]	23.23	7.89	4	5	837	95.6	7.27
P12382	6-phosphofructokinase, liver type [K6PL_MOUSE]	23.23	7.05	4	5	780	85.3	7.17
Q60865	Caprin-1 [CAPR1_MOUSE]	22.92	13.01	4	5	707	78.1	5.25
Q8BTV2	Cleavage and polyadenylation specificity factor subunit 7 [CPSF7_MOUSE]	22.32	7.64	2	4	471	52.0	8.00
P62482	Voltage-gated potassium channel subunit beta-2 [KCAB2_MOUSE]	21.96	17.44	4	5	367	41.0	9.00
Q6P5D3	Putative ATP-dependent RNA helicase DHX57 [DHX57_MOUSE]	21.31	5.62	5	5	1388	155.7	7.87
Q3TJZ6	Protein FAM98A [FA98A_MOUSE]	20.97	9.51	4	4	515	55.0	8.95
Q8R3C6	Probable RNA-binding protein 19 [RBM19_MOUSE]	20.64	7.25	5	5	952	106.0	6.57
Q6PHZ2	Calcium/calmodulin-dependent protein kinase type II subunit delta [KCC2D_MOUSE]	20.57	11.22	4	5	499	56.3	7.25
Q8VHN8	Protein syndesmos [SDOS_MOUSE]	20.45	29.38	5	5	211	23.4	9.26
P53996	Cellular nucleic acid-binding protein [CNBP_MOUSE]	20.33	28.65	3	4	178	19.6	7.58
Q99104	Myosin-Va [MYO5A_MOUSE]	19.12	2.59	3	4	1853	215.4	8.63
P62242	40S ribosomal protein S8 [RS8_MOUSE]	18.74	26.44	4	4	208	24.2	10.32
Q8BHN5	RNA-binding protein 45 [RBM45_MOUSE]	18.62	9.24	3	4	476	53.3	7.69
Q9D6Z1	Nucleolar protein 56 [NOP56_MOUSE]	18.00	10.69	4	4	580	64.4	9.14
P16858	Glyceraldehyde-3-phosphate dehydrogenase [G3P_MOUSE]	17.75	20.72	4	4	333	35.8	8.25
Q99JX7	Nuclear RNA export factor 1 [NXF1_MOUSE]	15.58	7.44	3	3	618	70.3	8.73
Q9JII5	DAZ-associated protein 1 [DAZP1_MOUSE]	15.45	11.58	3	3	406	43.2	8.56
Q8K310	Matrin-3 [MATR3_MOUSE]	15.32	6.62	3	3	846	94.6	6.25
Q8C2Q3	RNA-binding protein 14 [RBM14_MOUSE]	15.04	8.22	3	3	669	69.4	9.67
Q8CCS6	Polyadenylate-binding protein 2 [PABP2_MOUSE]	14.71	8.28	2	4	302	32.3	5.17
Q9CYR0	Single-stranded DNA-binding protein, mitochondrial [SSBP_MOUSE]	14.24	19.74	2	3	152	17.3	9.92
P29341	Polyadenylate-binding protein 1 [PABP1_MOUSE]	14.22	7.55	3	3	636	70.6	9.50
P11276	Fibronectin [FINC_MOUSE]	13.92	2.06	3	3	2477	272.3	5.59
Q8BZZ3	NEDD4-like E3 ubiquitin-protein ligase WWP1 [WWP1_MOUSE]	13.55	4.58	3	3	918	104.6	6.38
Q61510	E3 ubiquitin/ISG15 ligase TRIM25 [TRI25_MOUSE]	13.46	4.42	2	3	634	71.7	8.28
Q9ESX5	H/ACA ribonucleoprotein complex subunit 4 [DKC1_MOUSE]	13.15	9.43	3	3	509	57.4	9.28
P50096	Inosine-5'-monophosphate dehydrogenase 1 [IMDH1_MOUSE]	12.92	7.78	3	3	514	55.2	6.80
O88532	Zinc finger RNA-binding protein [ZFR_MOUSE]	12.24	2.79	2	3	1074	116.8	9.04
P98086	Complement C1q subcomponent subunit A [C1QA_MOUSE]	11.82	13.88	2	3	245	26.0	9.11
Q91W39	Nuclear receptor coactivator 5 [NCOA5_MOUSE]	11.82	8.12	2	2	579	65.3	9.82
Q8BL97	Serine/arginine-rich splicing factor 7 [SRSF7_MOUSE]	11.66	11.61	2	3	267	30.8	11.90
O70133	ATP-dependent RNA helicase A [DHX9_MOUSE]	11.22	2.75	3	3	1380	149.4	6.83
P62908	40S ribosomal protein S3 [RS3_MOUSE]	10.99	16.87	3	3	243	26.7	9.66
Q61545	RNA-binding protein EWS [EWS_MOUSE]	10.99	4.43	2	3	655	68.4	9.33

#: Number, PSM: peptide-spectrum match, AA: amino acid, MW: molecular weigh

Table S3. *Drosophila* Genotypes Used in this Study, Related to Experimental Procedures